DE GRUYTER OPEN

Numerical simulations of generation of high-energy ion beams driven by a petawatt femtosecond laser

Jarosław Domański,
Jan Badziak,
Sławomir Jabłoński

Abstract. This contribution presents results of a Particle-in-Cell simulation of ion beam acceleration via the interaction of a petawatt 25 fs laser pulse of high intensity (up to ~10^{21} W/cm^2) with thin hydrocarbon (CH) and erbium hydride (ErH$_3$) targets of equal areal mass density (of 0.6 g/m^2). A special attention is paid to the effect that the laser pulse polarization and the material composition of the target have on the maximum ion energies and the number of high energy (>10 MeV) protons. It is shown that both the mean and the maximum ion energies are higher for the linear polarization than for the circular one. A comparison of the maximum proton energies and the total number of protons generated from the CH and ErH$_3$ targets using a linearly polarized beam is presented. For the ErH$_3$ targets the maximum proton energies are higher and they reach 50 MeV for the laser pulse intensity of 10^{21} W/cm^2. The number of protons with energies higher than 10 MeV is an order of magnitude higher for the ErH$_3$ targets than that for the CH targets.

Key words: laser acceleration • laser plasma • ions • particle-in-cell simulations

J. Domański✉
Institute of Plasma Physics and Laser Microfusion (IPPLM),
23 Hery Str., 01-497 Warsaw, Poland
and Faculty of Physics,
Warsaw University of Technology,
75 Koszykowa Str., 00-662 Warsaw, Poland,
Tel.: +48 22 638 1460, Fax: +48 22 666 8372,
E-mail: jaroslaw.domanski@ifpilm.pl

J. Badziak, S. Jabłoński
Institute of Plasma Physics and Laser Microfusion (IPPLM),
23 Hery Str., 01-497 Warsaw, Poland

Introduction

Laser-driven generation of high-energy ion beams has recently attracted considerable interest due to a variety of potential applications including proton radiography, inertial confinement fusion (ICF) fast ignition, nuclear physics or hadron therapy [1–3].

The energy spectrum and the maximum energy of ion beam driven by a femtosecond laser show significant dependence on the laser intensity, the laser pulse polarization and the structure of the target, which in turn determines a dominant mechanism of ion acceleration. There are two main mechanisms of laser-driven ion acceleration for thin targets (thickness ≤100 μm): the target normal sheat acceleration (TNSA) [1, 2, 4–8] and the radiation presure acceleration (RPA) [7, 9, 10], also known as skin-layer ponderomotive acceleration (SLPA) [2, 11–13]. For linear polarization (LP) and moderate laser intensities the dominant acceleration mechanism is usually the TNSA. In this mechanism, an intense and short (below a few ps) laser pulse interacting with the front surface of the target produces plasma and fast electrons. The electrons penetrate through the target and at the target rear surface they form a Debye sheath playing the role of a virtual cathode.

A high electric field generated by this cathode $E_c \approx T_h/(eD_h)$ efficiently ionizes the surface atoms and accelerates the produced ions (T_h and D_h are the temperature and the Debye length of fast (hot) electrons). In the RPA scheme the ponderomotive force (the radiation pressure) created by the laser pulse near the critical plasma surface in front of the target drives forward and compresses the target plasma in a piston-like manner (the 'hole boring' stage). When the compressed plasma (ion bunch) reaches the target rear surface, it is detached from the target and accelerated further by the radiation pressure like a sail pushed by the wind (the 'light sail' stage). Previous studies presented in numerous papers investigated the effect of the laser beam polarization (circular polarization – CP vs. linear polarization – LP) [6, 14–16] on the generation of non-relativistic and relativistic proton beams from hydrogen and hydrocarbon plasma targets. Those studies show that for moderate and high laser intensities (I_L up to 10^{21} W/cm²) the TNSA model dominates for both types of polarization and that for ultra-high intensity RPA dominates (especially for CP [16]). Unfortunately, there are only few papers describing, especially in the high intensity regime, the influence of the target material and generation of ion beams from realistic two-species targets consisting of heavy atoms [6, 17, 18]. It should be noted that parameters of ion beams produced by TNSA and RPA mechanism significantly depend on the target thickness. The ion energies are inversely proportional to the thickness of the target up to a moment when the target becomes transparent to the laser pulse [6, 16].

In this paper, we will discuss the effect that the laser polarization and the target material have on the ion acceleration. The ion beams will be generated using hydrocarbon (CH) and erbium hydride (ErH_3) targets of an equal areal mass density (of 0.6 g/m²) irradiated by a 25 fs laser pulse of high intensity (I_L up to 10^{21} W/cm²). Both of the considered materials are easily available. The information about erbium hydride is available from American Elements Website [19]. We will concentrate on the maximum ion energies and the number of high energy (>10 MeV) protons. Using one-dimensional PIC simulations we will show that for the linear polarization the maximum and mean ion energies are higher than for the circular one. We will also prove that for ErH_3 targets the maximum proton energies and the numbers of high energy protons are significantly higher. The maximum proton energies achieve 50 MeV for the laser pulse intensity of 10^{21} W/cm² and the number of high energy protons is an order of magnitude higher for the ErH_3 targets than that for the CH targets.

Results and discussion

The numerical results presented in this paper were obtained using a one-dimensional relativistic PIC code [20], which is a modified version of the well known LPIC++ code [21]. The simulations were performed for a linearly (LP) or circularly polarized (CP) laser pulse of duration of 25 fs, of the intensity ranging from 10^{20} W·cm⁻² to 10^{21} W·cm⁻² and the wavelength of 800 nm. The laser pulse shape was described by a super-Gaussian function. Molecular densities of the targets corresponded to the solid state densities and they were equal to 4.86×10^{22} molecules/cm³ for CH and 2.69×10^{22} molecules/cm³ for ErH_3. In front of the target, a pre-plasma layer of 0.25 μm thickness and the density shape described by an exponential function was used and the ionization degrees of target components were assumed to be 6 for carbon and 10 for erbium (as it was assumed in [17]).

First, we will present results for different types of laser beam polarization. Plots are given showing maximum proton energy for CH targets (Fig. 1) and ErH_3 targets (Fig. 2). The data obtained for different beam polarizations are compared assuming equal laser energy fluence for both polarizations. For both types of polarization and for both types of target the maximum proton energy increases with an increase in the laser intensity. For LP the maximum energies of protons are much higher than those for CP and they achieve 25 MeV for the CH target and 50 MeV for the ErH_3 target. For CP the maximum proton energy reaches only 3 MeV both for CH and ErH_3 targets. This effect could be explained by the domination of the TNSA mechanism in the ion acceleration process. The energies of the fast electrons produced by the laser pulse on the front surface of the target depend on the maximum value of the electric and magnetic fields associated with the pulse. In the case of equal fluence of the laser energy for both polarizations this parameter is higher for the LP. According to the equation $E_c \approx T_h/(eD_h)$, a high electric field generated by the virtual cathode created by the fast electrons depends on the energy of these electrons and is higher for the linear polarization. As a result, the acceleration efficiency of ions is higher for the LP. This results match up with the previous results for the hydrogen and hydrocarbon targets and different laser intensities [6].

The following plots present a comparison of the maximum proton energies (Fig. 3) and the number of high energy protons (Fig. 4) for the CH and the ErH_3 targets for the linear polarization. In the case of the ErH_3 targets the maximum proton energies are higher and they reach 50 MeV for the laser pulse intensity of 10^{21} W/cm². The number of protons of energy higher than 10 MeV is an order of magnitude higher for the ErH_3 targets than that for the CH targets.

The observed differences in the parameters of protons generated using the CH and ErH_3 targets can be explained by the fact that interaction between ions and the laser beam – and the ion acceleration efficiency – depend on the q/m parameter (q – the ion charge, m – the ion mass). This parameter decreases with rising ion mass and as a result the interaction of heavier ions (like Er^{10+}) with the laser beam is weaker than interaction of lighter ions (like C^{6+}). During the process of acceleration particles create currents which weaken the electric and magnetic fields. For this reason, the laser beam interacting
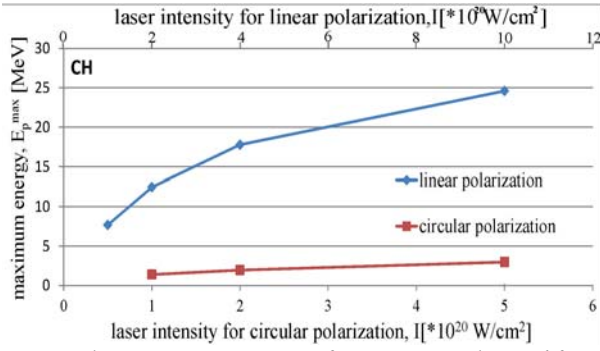
Fig. 1. The maximum energy of protons accelerated from the CH target, as a function of the laser intensity.
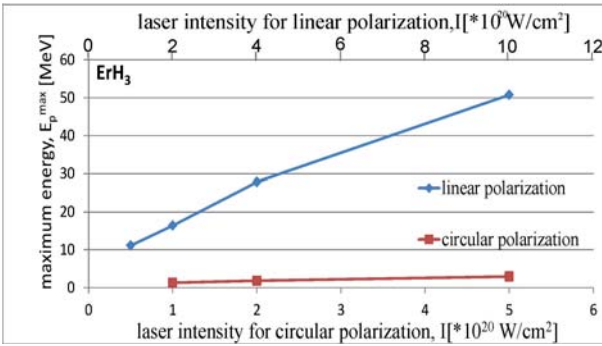

Fig. 2. The maximum energy of protons accelerated from the ErH$_3$ target, as a function of the laser intensity.
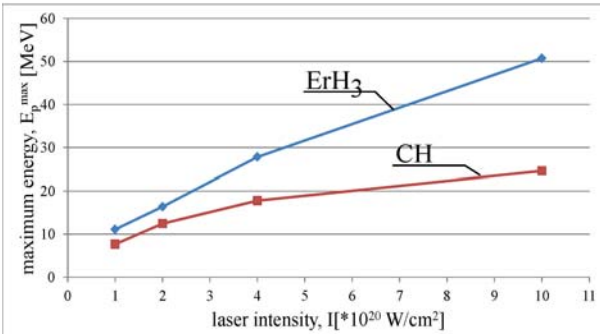

Fig. 3. The maximum energy of the laser-accelerated protons, as a function of the laser intensity.
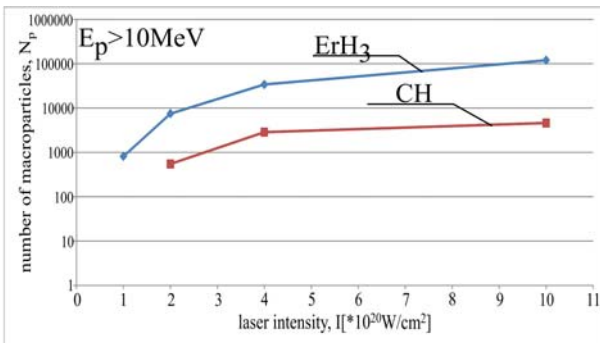

Fig. 4. The number of high energy (>10 MeV) protons, as a function of the laser intensity.

Fig. 5. The charge density for the ErH$_3$ target (a) and the CH target (b); the laser pulse intensity is 10^{21} W/cm^2.

with protons can be described as the initial beam minus a screening factor which comes from other particles. For ErH$_3$ target the screening factor which comes from the Er ions is quite low and as a result in the early stages of interaction protons are accelerated more efficiently. The global current density generated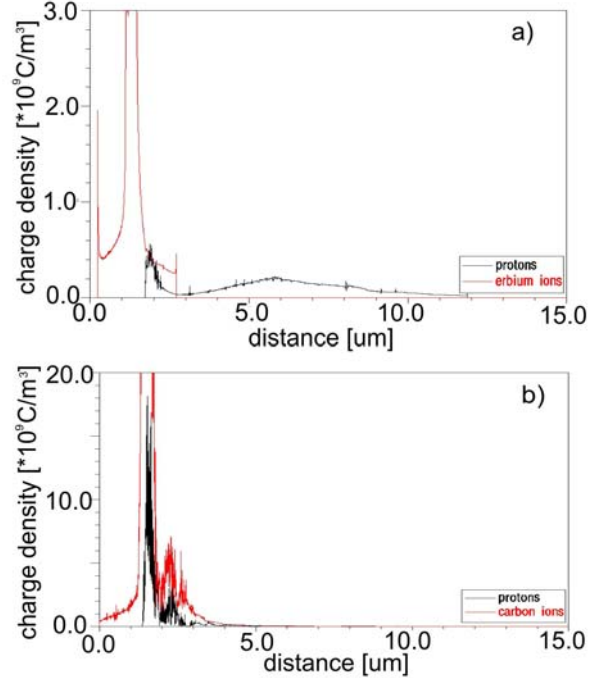 by the C^{6+} ions at the laser pulse intensity of 10^{21} W/cm^2 reaches 2.4×10^{19} A/m^2 while for Er^{10+} only 2.9×10^{18} A/m^2. In the simulation showing the higher efficiency of proton acceleration off the ErH$_3$ target the spatial separation between protons and erbium ions is visible (Fig. 5a). For the CH target the separation is not visible (Fig. 5b). These results match up with the previous results obtained for lower laser intensities [17].

Conclusions

It is shown that the laser light polarization has a significant influence on the ion acceleration, both for targets composed of light and heavy ions. For the linear polarization the maximum energy of protons is higher than that for the circular one. The maximum energies of protons and the number of highly energetic protons show significant dependence on the target composition. The maximum proton energies are higher in the case of the ErH$_3$ targets than in the case of the CH targets and they reach 50 MeV for the laser pulse intensity of 10^{21} W/cm^2. The number of protons with the energy higher than 10 MeV is an order of magnitude higher for the ErH$_3$ targets than that for the CH targets.

References

1. Borghesi, M., Fuchs, J., Bulanov, S. V., MacKinnon, A. J., Patel, P. K., & Roth, M. (2006). Fast ion generation by high-intensity laser irradiation of solid targets and applications. *Fusion Sci. Technol.*, *49*, 412 [and references therein].
2. Badziak, J. (2007). Laser-driven generation of fast particles. *Opto-Electron. Rev.*, *15*, 1. DOI: 10.2478/s11772-006-0048-3 [and references therein].

3. Ledingham, K. W. D., & Galster, W. (2010). Laser-
-driven particle and photon beams and some applica-
tions. *New J. Phys.*, *12*, 045005. DOI:10.1088/1367-
2630/12/4/045005.

4. Wilks, S. C., Langdon, A. B., Cowan, T. E., Roth,
M., Singh, M., Hatchett, S., Key, M. H., Penning-
ton, D., MacKinnon, A., & Snavely, R. A. (2001).
Energetic proton generation in ultra-intense laser–
–solid interactions. *Phys. Plasmas*, *8*, 542. DOI:
10.1063/1.1333697.

5. Zani, A., Sgattoni, A., & Passoni, M. (2011). Paramet-
ric investigations of target normal sheath acceleration
experiments. *Nucl. Instrum. Methods Phys. Res. Sect.
A-Accel. Spectrom. Dect. Assoc. Equip.*, *653*, 94–97.

6. Daido, H., Nishiuchi, M., & Pirozhkov, A. S. (2012).
Review of laser-driven ion sources and their ap-
plications. *Rep. Prog. Phys.*, *75*, 056401. DOI:
10.1088/0034-4885/75/5/056401.

7. Macchi, A., Borghesi, M., & Passoni, M. (2013). Ion
acceleration by superintense laser-plasma interaction.
Rev. Mod. Phys., *85*, 751.

8. Passoni, M., Bertagna, L., & Zani, L. (2010). Target
normal sheath acceleration: theory, comparison with
experiments and future perspectives. *New J. Phys.*,
12, 045012.

9. Esirkepov, T., Borghesi, M., Bulanov, S. V., Mourou,
G., & Tajima, T. (2004). Highly efficient relativistic-
ion generation in the laser-piston regime. *Phys.
Rev. Lett.*, *92*, 175003. DOI: 10.1103/PhysRev-
Lett.92.175003.

10. Macchi, A., Cattani, F., Liseykina, T. V., & Cornolti,
F. (2005). Laser acceleration of ion bunches at the
front surface of overdense plasmas. *Phys. Rev. Lett.*,
94, 165003. DOI: 10.1103/PhysRevLett.94.165003.

11. Badziak, J., Hora, H., Woryna, E., Jabłoński, S., Laśka,
L., Parys, P., Rohlena, K., & Wołowski, J. (2003).
Experimental evidence of differences in properties
of fast ion fluxes from short-pulse and long-pulse
laser–plasma interactions. *Phys. Lett. A, 315*, 452.
DOI: 10.1016/S0375-9601(03)01101-0.

12. Badziak, J., Jabłoński, S., Parys, P., Rosiński, M.,
Wołowski, J., Szydłowski, A., Antici, P., Fuchs, J., &
Mancic, A. (2008). Ultraintense proton beams from
laser-induced skin-layer ponderomotive acceleration.
J. Appl. Phys., *104*, 063310. DOI: 10.1063/1.2981199.

13. Badziak, J., Mishra, G., Gupta, N. K., & Holkund-
kar, A. R. (2011). Generation of ultraintense proton
beams by multi-ps circularly polarized laser pulses for
fast ignition-related applications. *Phys. Plasmas*, *18*,
053108. DOI: 10.1063/1.3590856.

14. Liseykina, T. V., & Macchi, A. (2007). Features of ion
acceleration by circularly polarized laser pulses. *Appl.
Phys. Lett.*, *91*, 171502. DOI: 10.1063/1.2803318.

15. Klimo, O., Psikal, J., Limpouch, J., & Tikhonchuk,
V. T. (2008). Monoenergetic ion beams from ultra-
thin foils irradiated by ultrahigh-contrast circularly
polarized laser pulses. *Phys. Rev. Spect. Top.-Accel.
Beams*, *11*, 031301.

16. Domański, J., Badziak, J., & Jabłoński, S. (2013).
Effect of laser light polarization on generation of
relativistic ion beams driven by an ultraintense laser.
J. Appl. Phys., *113*, 173302.

17. Foord, M. E., Mackinnon, A. J., Patel, P. K., MacPhee,
A. G., Ping, Y., Tabak, M., & Town, R. P. J. (2008).
Enhanced proton production from hydride-coated
foils. *J. Appl. Phys.*, *103*, 056106.

18. Domański, J., Badziak, J., & Jabłoński, S. (2014).
Particle-in-cell simulation of acceleration of ions to
GeV energies in the interactions of an ultra-intense
laser pulse with two-species targets. *Phys. Scripta,
T161*, 014030.

19. www.americanelements.com/erhid.html.

20. Badziak, J., & Jabłonski, S. (2010). Ultraintense ion
beams driven by a short-wavelength short-pulse laser.
Phys. Plasmas, *17*, 073106. DOI: 10.1063/1.3458900.

21. Lichters, R., Pfund, R. E. W., & Meyer-Ter-Vehn,
J. (1997). *LPIC++, A parallel one-dimensional
relativistic electromagnetic particle-in-cell code for
simulating laser-plasma-interaction*. Garching: Max-
-Planck-Institut für Quantenoptik. (MPQ 225). www.
lichters.net/download.html.